Electrotransport Characteristics of Ceramic and Single Crystal Materials with the $(ZrO_2)_{0.89}(Sc_2O_3)_{0.10}(Y_2O_3)_{0.01}$ Composition[1]

I. E. Kuritsyna[a, *], **S. I. Bredikhin**[a], **D. A. Agarkov**[a], **M. A. Borik**[b], **A. V. Kulebyakin**[b],
F. O. Milovich[c], **E. E. Lomonova**[b], **V. A. Myzina**[b], and **N. Yu. Tabachkova**[c]

[a]*Institute of Solid State Physics, Russian Academy of Sciences, Chernogolovka, Moscow oblast, 142432 Russia*
[b]*Prokhorov Institute of General Physics, Russian Academy of Sciences, Moscow, 119991 Russia*
[c]*Moscow Institute of Steel and Alloys, Moscow, 119049 Russia*
*e-mail: koneva@issp.ac.ru

Abstract—The comparative analysis of electrotransport characteristics and structure of ceramic and single-crystal solid electrolytes with the $(ZrO_2)_{0.89}(Sc_2O_3)_{0.10}(Y_2O_3)_{0.01}$ composition is carried out before and after their life tests. It is shown that before the life tests, the specific conductivities of single-crystal and ceramic materials virtually coincide. During the 3000 h life tests, the specific ionic conductivity decreases for both single crystal and ceramic samples down to about 0.1 S cm^{-1} but the degradation of conductivity in single crystal proceeds more slowly as compared with the ceramic material. The reason for degradation of electrotransport characteristics in the single crystal is associated with the transition of its bulk structure from the t'' phase to a phase with the higher degree of tetragonality, whereas in the ceramic material, in addition to the latter process, a rhombohedral phase appears presumably along grain boundaries.

Keywords: ionic conductivity, stabilized zirconia, single crystals, life tests

INTRODUCTION

Among zirconia-based ceramic materials codoped with scandia and yttria, the highest ionic conductivity is demonstrated by the solid electrolyte containing 10 mol % Sc_2O_3 and 1 mol % Y_2O_3 (10Sc1YSZ) [1, 2]. However, ceramic materials are characterized by a wide scatter of conductivity determined by the ceramics synthesis. The conductivity may depend on the grain size, pores, the presence of additional (foreign) impurities in initial materials. These factors affect both the bulk and grain-boundary conductivity of ceramics changing their ratio. The smaller the grain size, the larger contribution is made by the grain-boundary conductivity. Experimental and theoretical studies of the diffusion of oxygen ions along grain boundaries in a cubic solid solution based on zirconia showed that the diffusion rate is different in the bulk and surface regions [3–8]. Molecular dynamics simulations have shown [3, 4] that in the system ZrO_2– 8 mol % Y_2O_3, the grain boundary acts as the source of resistance to the diffusion of oxygen ions. This effect strengthens in the presence of dopant segregation in the grain boundary region because the vacancies required for the transfer of anions are localized in the grain boundary region due to association with dopant ions. However, it was noted that depending on the synthetic conditions and composition of the solid electrolyte, the conductivity of boundaries may turn out to be higher than the bulk conductivity as a result of their different compositions. For instance, this situation is observed when zirconia is codoped with scandia and ceria [7, 8].

The drawbacks of solid electrolytes based on zirconia include degradation of ionic conductivity during the work of solid oxide fuel cells (SOFC). The degradation of electrotransport properties of solid electrolytes is mainly studied on ceramic samples for which the decrease in ionic conductivity may be associated with the phase transformations occurring in the high temperature region and/or the segregation of admixtures at grain boundaries and also with the changes in the grain size (recrystallization). In contrast to ceramics, synthesizing materials in the form of single crystals makes it possible to eliminate the effect of certain factors, such as grain size, distribution of solid-solution components in the volume and boundaries of grains, and intergrain stresses, on the electrophysical characteristics of the material and also on the changes in these characteristics at high temperatures close to those of SOFC operation. Thus, studying single crys-

---

[1] Presented at the IV All-Russian Conference "Fuel Cells and Fuel Cell based Power Plants" (with international participation) June 25–29, 2017, Suzdal, Vladimir region.
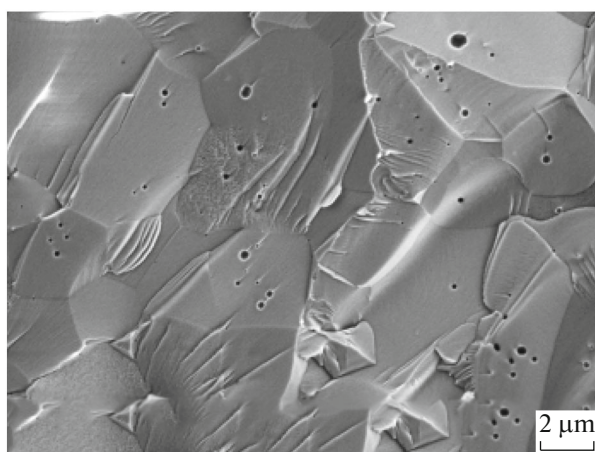
Fig. 1. Surface image of cross section of 10Sc1YSZ ceramic sample.

tals may allow one to assess the contribution of the bulk component of solid electrolyte conductivity by excluding the contribution of the grain-boundary conductivity and assess the effect of conditions of fuel-cell operation on the bulk characteristics of material.

The goal of this study is to compare the electro-transport characteristics and structure of ceramic and single-crystal materials of the 10Sc1YSZ composition in the course of life tests at SOFC working temperatures.

EXPERIMENTAL

10Sc1YSZ single crystals were grown by targeted crystallization of the melt in a cool container. The crystals were grown on the setup Kristall-407 (Russia) in a cool container with the diameter of 130 mm at the growth rate of 10 mm/h. For the load, we used powders of zirconia, scandia, and yttria with the main substance content of no less than 99.99%. Ceramic samples 10Sc1YSZ were obtained by uniaxial pressing of commercial powder (Daiichi Kigenso Kagaku Kogyo, Japan). After this, the samples were sintered in air atmosphere at 1520°C for 7 h.

The microstructure of samples was studied on a scanning electron microscope of high resolution SUPRA 50VP (Carl Zeiss, Germany) with microanalysis system INCA Energy+ (Oxford). The analysis of distribution of scandia and yttria along the crystal length was determined by energy-dispersive analysis. The phase composition of samples was controlled by X-ray diffraction method on Bruker D8 diffractometer (Germany) in CuK_{α} radiation and also by Raman spectroscopy on microscope-spectrograph Renishaw inVia (UK).

For studying ionic conductivity, the plates measuring 7×7 mm with the thickness of 500 μm were cut out from 10Sc1YSZ samples. On both sides of these plates, platinum paste was placed and cosintered at 950°C for 1 h.

The bulk conductivity was calculated from impedance data. These measurements were carried out on the analyzer of frequency characteristics Solartron SI 1260 (Solartron Analytical, UK) in the frequency range from 100 mHz to 3 MHz with the amplitude of applied alternating signal of 24 mV in the temperature interval of 350–900°C in air. The life tests of ceramic and single-crystal 10Sc1YSZ samples were carried out at 850°C for 3000 h in air medium. The impedance spectra were processed with the use of ZView software (ver. 2.8). The bulk resistance of crystals (R_b) was calculated in terms of the following equivalent circuit: $(R_b - CPE_b)(R_{electrode} - CPE_{electrode})$ at low temperatures of 350–500°C. For polycrystals, the bulk resistance was calculated in terms of the following equivalent circuits: $(R_b - CPE_b)(R_{gb} - CPE_{gb})(R_{electrode} - CPE_{electrode})$ and $LR_b(R_{electrode} - CPE_{electrode})$, where $R_{electrode}$ is the resistance of the electrode/electrolyte interface, $CPE_{electrode}$ is the constant phase element characterizing the processes at the electrode interface, R_{gb} is the grain boundary resistance, CPE_{gb} is the constant phase element characterizing the processes at grain boundaries, L is the inductance of current leads.

RESULTS AND DISCUSSION

10Sc1YSZ single crystals were optically uniform, transparent, without visible defects. No light scattering was observed, which suggests that neither second phase nor twin structure were present in the crystal volume. 10Sc1YSZ ceramic samples were well sintered and had no open pores. The grain size was from 1 to 5 μm. Figure 1 shows an image of a section of 10Sc1YSZ ceramic sample. The presence of fine closed pores in the volume of individual grains deserves mention.

The analysis of scandia and yttria distribution along the single-crystal length shows that the crystal composition was uniform and the concentration of scandia and yttria virtually corresponded to their content in the original load (Fig. 2).

The X-ray diffraction (XRD) study of industrial powder, ceramic samples, and crystals with the 10Sc1YSZ composition showed that all of them were monophase with the cubic structure of fluorite. The phase composition was also controlled by the Raman method. Figure 3 shows Raman spectra for single-crystal and ceramic 10Sc1YSZ samples. The spectra of ceramic and single-crystal 10Sc1YSZ samples contain a peak in the vicinity of 480 cm^{-1} which corresponds to the *t*″ phase. The latter has the degree of tetragonality $c/a = 1$ [9] but belongs to the symmetry space group $P4_2/nmc$ due to a small shift of oxygen atoms in the anionic sublattice along the C axis [2, 10]. Thus, the comparison of XRD and Raman data on the phase composition showed that both 10Sc1YSZ single crys-
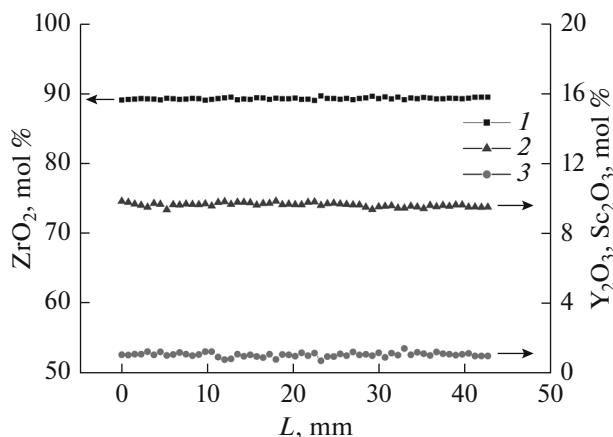
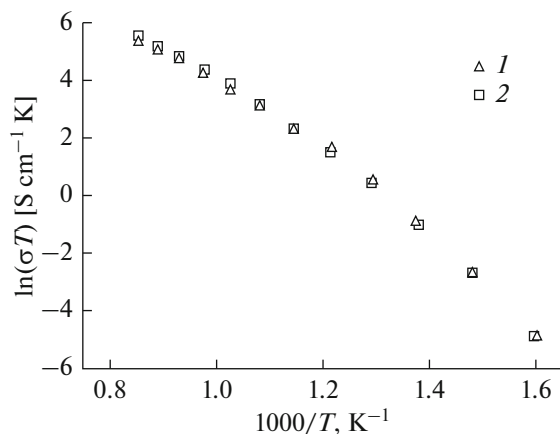**Fig. 2.** Distribution of oxides along the length of 10Sc1YSZ single crystal: (*1*) ZrO_2, (*2*) Sc_2O_3, (*3*) Y_2O_3.

Fig. 3. Raman spectra of original 10Sc1YSZ samples: (*1*) single crystal, (*2*) polycrystal.

Fig. 4. Temperature dependences of specific conductivity of 10Sc1YSZ samples: (*1*) single crystal, (*2*) polycrystal.
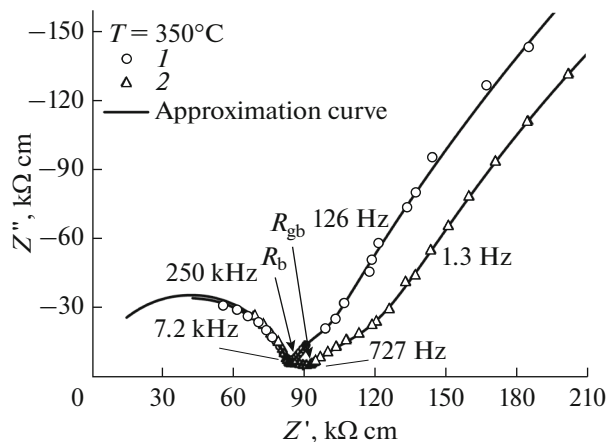
Fig. 5. Impedance spectra of 10Sc1YSZ samples measured at 350°C in air: (*1*) single crystal, (*2*) polycrystal.

tals and ceramic samples which were identified by XDR studies as cubic had in fact the tetragonal structure of the *t*″ phase. In contrast to tetragonal phases *t* and *t*′, the *t*″ phase structure is characterized by the absence of twins. This is clearly seen for the grown single crystals which do not differ from cubic crystals in their appearance but their Raman spectrum is close to that of tetragonal crystals.

Figure 4 shows the temperature dependences of the specific bulk conductivity of single crystal and ceramic 10Sc1YSZ samples. These dependences are linear. It deserves mention that the ionic conductivities of samples virtually coincide (the scatter fits the error limits). Such behavior is clearly demonstrated by the form of impedance spectra for sample studied (Fig. 5). The hodograph of a polycrystalline sample contains an additional arc which corresponds to the grain-boundary resistance; as the temperature increases, the grain-boundary resistance of the polycrystalline sample
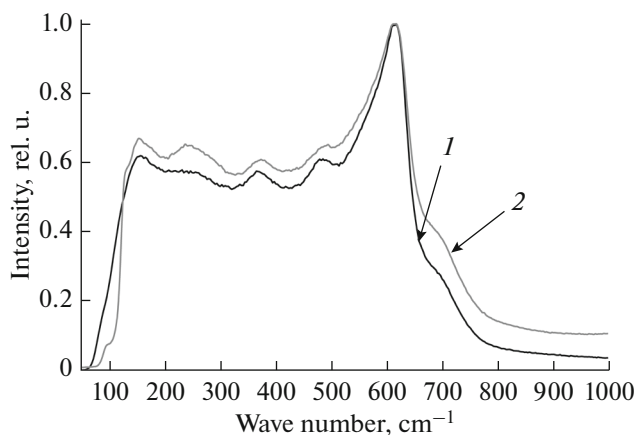
decreases so that the arc part corresponding to grain boundary transport becomes invisible.

For 10Sc1YSZ samples, the life tests were carried out at 850°C. They demonstrated that during 3000 h, the specific ionic conductivity decreased for both single crystal and ceramic samples down to ca. 0.1 S cm^{-1} (Fig. 6). For 3000 h life tests, the ceramic and single crystal materials underwent degradation but at different rates. For the ceramic material, the conductivity decreased sharply down to 0.1 S cm^{-1} during 150–200 h and remained virtually constant in the rest period. The conductivity of the single crystal sample decayed to ca. 0.1 S cm^{-1} during 1500–2000 h. The data obtained showed that the changes causing the degradation of conductivity occurred in the single crystal much more slowly than in the ceramic sample. The different rate of conductivity degradation for single crystal and polycrystalline 10Sc1YSZ samples is probably associated with the fact that, in addition to the effect of
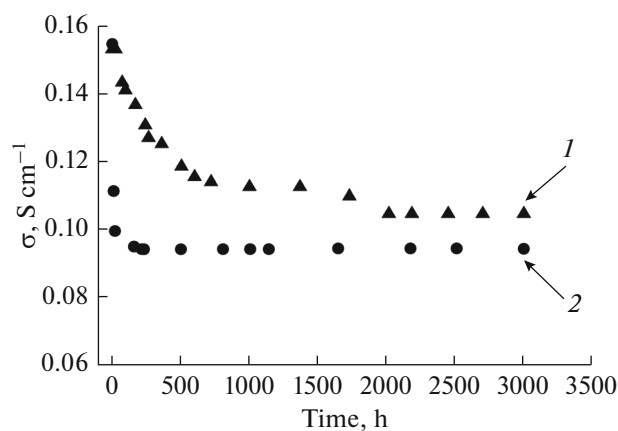
Fig. 6. Time dependences of the specific bulk conductivity of 10Sc1YSZ membranes exposed at 850°C for 3000 h in air: (*1*) single crystal, (*2*) polycrystal.

Fig. 7. Raman spectra of 10Sc1YSZ samples after life tests: (*1*) single crystal, (*2*) polycrystal.

changes in the bulk conductivity, the degradation of ceramic material is determined also by the changes in the grain boundary component of conductivity, i.e., by the processes at grain boundaries.

The XRD studies of the phase composition of single crystal and ceramic 10Sc1YSZ samples subjected to life tests have shown that the phase composition of samples remains unchanged and both materials retain the cubic structure of fluorite. But the Raman method, being more sensitive with respect to phase composition variations, in particular, to the changes in the oxygen position in the structure of materials, revealed that the structure of single crystal and ceramic samples changed differently during the life tests. Figure 7 shows the Raman spectra for single crystal and ceramic 10Sc1YSZ materials after life tests. In the single crystal, the Raman spectrum approaches the spectrum of a tetragonal single crystal [10], which is indicated by the shift of the 616 cm^{-1} band to 626 cm^{-1} and the increase in intensity of band at 252 cm^{-1}, which suggests that oxygen atoms in the anionic sublattice shift further along the C axis. The structure of the t'' phase shifts towards the higher degree of tetragonality. For the ceramic materials, the changes in the Raman spectrum after the life tests can be attributed to the appearance of a rhombohedral phase in addition to the original cubic phase. Thus, after the life tests, in the Raman spectrum of the ceramic material, the band at 616 cm^{-1} shifted slightly to 612 cm^{-1}; moreover, the broadening of this band in the region of 520–590 cm^{-1} occurred. In addition, a band at 312 cm^{-1} appeared which is typical of the rhombohedral phase [11] and was absent in the initial Raman spectrum of the ceramic sample before life tests.

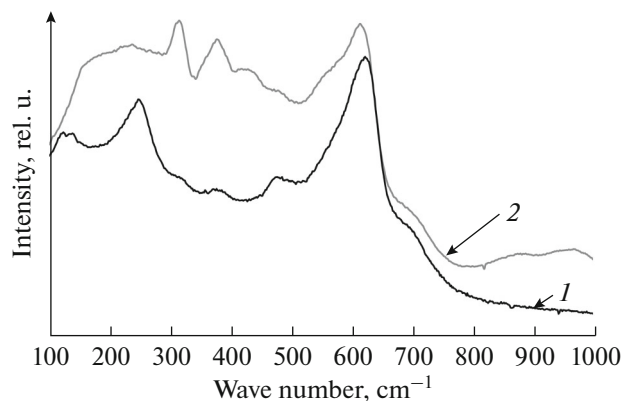Thus, it can be assumed that in the ceramic 10Sc1YSZ material, various structural changes occur in the material bulk and along grain boundaries. In grain's bulk, the changes that occur during life tests are similar to those observed in the structure of the 10Sc1YSZ single crystal. Namely, as a result of ordering of vacancies and the changes in the environment of cations of zirconium, scandium, and yttrium, the shift of oxygen atoms within anionic sublattice along C axis occurs which correlates with the ionic radii of these cations. Apparently, at grain boundaries, the concentration of stabilizing oxides is observed to increase both after the synthesis because of the nonuniform distribution of solid solution components and at elevated temperatures of life tests as a result of diffusion of cations of stabilizing oxides. The increase in the overall concentration of stabilizing oxides may result in a partial transition of the original t'' phase to the rhombohendral phase [2, 9–11].

By comparing the information on how the electrotransport characteristics of single-crystal and ceramic 10Sc1YSZ materials change during the life tests with the data on the changes in the phase composition of these samples before and after the tests it is possible to associate the degradation of electrotransport characteristics with the transition of the material bulk structure from t'' phase to the more tetragonal phase as a result of the shift of oxygen atoms along the c axis. In the ceramic material, this is also associated with the appearance of a rhombohedral phase presumably along grain boundaries.

The different rates of conductivity degradation in single-crystal and ceramic samples may be associated with the fact that the transition of the material bulk structure from t'' phase to a phase with the higher degree of tetragonality is a long-term process as compared with the changes that occur at grain boundaries. Thus, in the first stage of degradation, the key role is played by the processes at grain boundaries caused by nonuniformity of distribution of solid solution components or, probably, due to the presence of foreign admixtures.

CONCLUSIONS

The structure and electrophysical characteristics of the 10Sc1YSZ solid solution that exhibits the highest oxygen-ion conductivity among materials based on zirconia codoped with scandia and yttria are compared for single-crystal and ceramic samples. It is shown that before life tests, the specific conductivity of single-crystal and ceramic 10Sc1YSZ samples is virtually the same. During 300 h life tests, the specific ionic conductivity decreases for both single crystal and ceramic samples down to ca. 0.1 S cm^{-1}, but the degradation rates of these materials are different. The conductivity of single crystal degrades much more slowly as compared with ceramic material. It is shown that during long-term thermal treatment, the oxygen atoms in the anionic sublattice shift along the C axis. This transforms the original t''-phase structure to the more tetragonal structure. In addition, in the ceramic material after life tests, the rhombohedral phase appears presumably along grain boundaries. The different rates of conductivity degradation in single crystal and ceramic samples may be associated with the fact that the transition of the t'' phase structure to a phase with the higher degree of tetragonality is the slower process than the changes that occur along grain boundaries and are associated with the rhombohedral phase appearance.

ACKNOWLEDGMENTS

REFERENCES

1. Politova, T.I. and Irvine, J.T.S., Investigation of scandia–yttria–zirconia system as an electrolyte material for intermediate temperature fuel cells—influence of yttria content in system $(Y_2O_3)_x(Sc_2O_3)_{(11-x)}(ZrO_2)_{89}$, *Solid State Ionics*, 2004, vol. 168, p. 153.

2. Borik, M.A., Bredikhin, S.I., Bublik, V.T., Kulebyakin, A.V., Kuritsyna, I.E., Lomonova, E.E., Milovich, F.O., Myzina, V.A., Osiko, V.V., Ryabochkina, P.A., Seryakov, S.V., and Tabachkova, N.Y., Phase composition, structure and properties of $(ZrO_2)_{1-x-y}(Sc_2O_3)_x(Y_2O_3)_y$ solid solution crystals ($x = 0.08$–0.11; $y = 0.01$–0.02) grown by directional crystallization of the melt, *J. Crystal Growth*, 2017, vol. 457, p. 122.

3. Fisher, C.A.J. and Matsubara, H., Oxide ion diffusion along grain boundaries in zirconia: A molecular dynamics study, *Solid State Ionics*, 1998, vol. 113, p. 311.

4. Verkerk, M.J., Middelhuis, B.J., and Burggraaf, A.J., Effect of grain boundaries on the conductivity of high-purity ZrO_2–Y_2O_3 ceramics, *Solid State Ionics*, 1982, vol. 6, p. 159.

5. Vaßen, R., Stöver D., de Haart, L.G.J., and Cappadonia, M., Grain size-dependent electrical conductivity of polycrystalline cerium oxide: I. Experiments, *Brit. Ceram. Proc.*, 1996, vol. 56, p. 35.

6. Brossmann, U., Knoner, G., Schaefer, H.-E., and Wurschum, R., Oxygen diffusion in nanocrystalline ZrO_2, *Adv. Mater. Sci.*, 2004, vol. 6, p. 7.

7. Preis, W., Waldhäusla, J., Egger, A., Sitte, W., de Carvalho, E., and Irvine, J.T.S., Electrical properties of bulk and grain boundaries of scandia-stabilized zirconia co-doped with yttria and ceria, *Solid State Ionics*, 2011, vol. 192, p. 148.

8. Kumar, A., Jaiswal, A., Sanbui, M., and Omar, S., Oxygen-ion conduction in scandia-stabilized zirconia-ceria solid electrolyte (xSc_2O_3–$1CeO_2$–$(99-x)ZrO_2$, $5 \leq x \leq 11$), *J. Amer. Ceram. Soc.*, 2016, vol. 99, p. 1.

9. Yashima, M., Sasaki, S., Kakihana, M., Yamaguchi, Y., Arashi, H., and Yoshimura, M., Oxygen-induced structural change of the tetragonal phase around the tetragonal-cubic phase boundary in ZrO_2–$YO_{1.5}$ solid solutions, *Acta Crystallogr. Sect. B: Struct. Sci.*, 1994, vol. 50, p. 663.

10. Borik, M.A., Bredikhin, S.I., Kulebyakin, A.V., Kuritsyna, I.E., Lomonova, E.E., Milovich, F.O., Myzina, V.A., Osiko, V.A., Seryakov, S.V., and Tabachkova, N.Yu., Structure and properties of the crystals of solid electrolytes $(ZrO_2)_{1-x-y}(Sc_2O_3)_x(Y_2O_3)_y$ ($x = 0.035$–0.11, $y = 0$–0.02) prepared by selective melt crystallization, *Russ. J. Electrochem.*, 2016, vol. 52, p. 655.

11. Borik, M.A., Bredikhin, S.I., Kulebyakin, A.V., Kuritsyna, I.E., Lomonova, E.E., Milovich, F.O., Myzina, V.A., Osiko, V.V., Panov, V.A., Ryabochkina, P.A., Seryakov, S.V., and Tabachkova, N.Yu., Melt growth, structure and properties of $(ZrO_2)_{1-x}(Sc_2O_3)_x$ solid solution crystals ($x = 0.035$–0.11), *J. Crystal Growth*, 2016, vol. 443, p. 54.

Translated by T. Safonova